# Seismic performance of unreinforced masonry buildings: application to Barcelona, Spain

**J.A. Avila-Haro, J.R. González-Drigo, Y.F. Vargas, L.G. Pujades & A.H. Barbat**
*Technnical University of Catalonia, Spain*

**S. Cattari**
*University of Genoa, Italy*

**SUMMARY:**
In 1856, the city of Barcelona started its extension (Eixample in Catalan) due to various reasons. The Eixample district occupies the central part of the city over a wide area of 7,46 km2. In absolute terms, it is the most populated district of Spain. Nearly half of the buildings of this district were built before 1940, and approximately the 65% of them were constructed with unreinforced masonry (URM) of ceramic bricks, without any consideration of the seismic action. These structures were built as a part of an orthogonal aggregate. Each aggregate includes approximately twenty buildings.

The buildings, usually with an orthogonal plan, have considerable heights and an important number of large openings in their façades and inner walls. Among the most typical features of these buildings we can find the presence of very long intermediate walls without any reinforcement; slabs with joists that, according to the year of construction, were made of wood, steel or precast concrete, completed with ceramic brick vaults.

The purpose of this paper is to evaluate the capacity and fragility of a sufficiently characteristic set of buildings of the Eixample district of Barcelona, modelled individually and as an aggregate, with their most representative geometric and mechanical parameters.

Several push-over analyses were performed using the TreMuri software and the fragility of the buildings was evaluated according to the Risk-UE project. The correspondent comparisons between the individual results and the aggregate ones are presented.

*Keywords: Barcelona, unreinforced masonry, push-over analysis, fragility, damage index*

## 1. INTRODUCTION

Due to their elevated population densities, the modern cities of the Mediterranean basin enclose a large stock of buildings and infrastructures, including a huge amount of structures with more than 100 years which are still being used for different purposes.

According to their location, the structural typology and the construction materials, procedures and period, the seismic vulnerability and the behavior of this set of structures varies widely. Thus, it is important to consider the seismic hazard attached to them (Jimenez et al., 2001).

Because of this, the studies on the field of seismic engineering have been aimed to the development and application of procedures in order to enhance the seismic behaviour of structures. There are several procedures and techniques for this purpose, having different objectives and levels of resources and time consumption (Barbat et al., 2006; Carreño et al., 2007; Barbat et al., 2008; Lantada et al., 2009; Pujades et al.,2012).

One of the Mediterranean basin cities with a high stock of ancient buildings is Barcelona. Barcelona is a city located in the western Mediterranean Sea, in a low-to-moderate seismic region of the Iberian Peninsula. Its establishment can be attributed to the roman emperor Augustus between the 15 to 10 years B.C. Among several centuries, the city passed into the hands of various empires and governments, being highly prized because of its strategic location and its commercial port.

Like many other cities in that time it was surrounded by walls in order to protect it from several attacks. These walls were expanded up to two times in order to enclose the established villages around them and also to increase the buildable area trying to solve the elevated population density problem.

It is in the mid-19$^{th}$ century when, due to the high population density and limited availability of space within the walls, when the government decides to finally bring down the walls and allow the expansion of the city. This enlargement (Eixample in Catalan) will follow the guidelines of the project designed by the civil engineer Ildefonso Cerdà, which with a remarkable urban vision will settle the basis for its construction.

During the first period of expansion, approximately between 1860 and 1940, the majority of the constructed buildings were built with unreinforced masonry and without any seismic consideration. Nowadays a large amount of these buildings are still used as dwellings, having more than 100 years of existence. In this way, the vulnerability of the unreinforced masonry structures added to the high population and the low but existing seismic hazard of the zone, have increased the seismic risk in this urban area (Lantada, 2007).

The buildings were not only built as isolated structures, in many cases they were built as a set of buildings that formed and aggregate, constituting the so called blocks or apples. The main objective of this work is to assess the vulnerability and seismic risk of these buildings, as individual and as an aggregate, following the guidelines proposed by the Risk-UE project.

## 2. URBAN PROJECT

It was until 1854 when the decree to demolish the walls surrounding the city of Barcelona was promulgated. Thus, the urbanization of the plain between the walls, the coast and the Collserola Mountains was permitted.

The local government organized a contest in order to find the project that could solve in the best way the need to expand the city. However, the central government gave the project to the civil engineer Ildefonso Cerdà, causing some opposition from local government reflected in the changes made to some of the ideas of the original project. The Cerdà project included not only issues of urbanization, it also included aspects of health, mobility and transportations inside and outside the city, as well as social and welfare aspects.

Queen Elizabeth II placed the first stone on September 4, 1860. The new district was named Eixample (enlargement). The 15% of the population of the city live in the Eixample district, containing approximately 12% of the total housing stock. The unreinforced masonry (URM) buildings represent almost 70% of all buildings in the Eixample district (Lantada, 2007). Most of the URM buildings were constructed before 1960 (when the reinforced concrete was fully introduced for construction), and their average year of construction is 1931.

Quadrangular blocks with an average of 133 meters per side constitute the block reticule that defines the urban framework of the Eixample district. Blocks are separated by 20-25 meters streets from each other. Two main types of buildings can be identified in each block, those located in the centre of each of the four sides of the block, presenting a rectangular perimeter, and those with a pentagonal perimeter, located in the corners of the blocks (See Fig. 2.1).

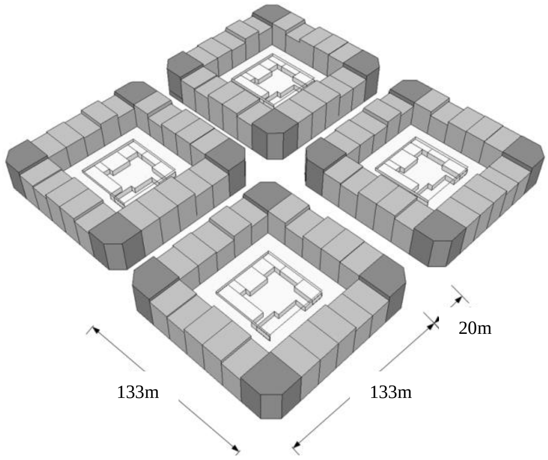


**Figure 2.1.** Block reticule of the urban framework of the Eixample district in Barcelona, Spain

## 3. BUILDINGS

The analyzed buildings correspond to a section of a block located in the Eixample district. The studied isolated buildings will be identified as M153, M155, M157 and M159, and the aggregate is composed of the first two isolated buildings which result to be identical (See Fig. 3.1). Each building present two main analysis directions (+X and +Y).

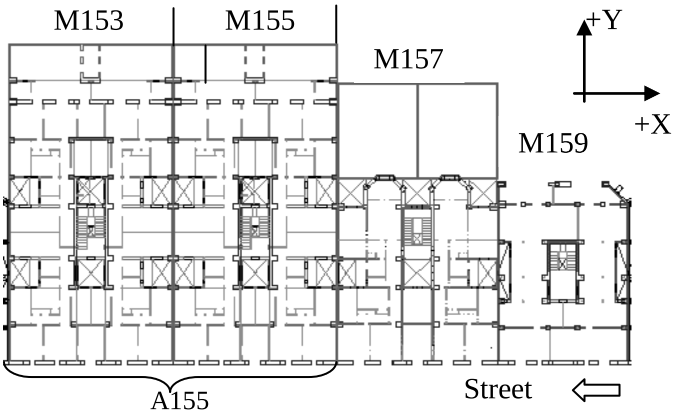


**Figure 3.1.** Floor plan of the studied row of buildings located in Barcelona, Spain

These buildings were selected due to their good representativeness of the typical characteristics of the Eixample's URM buildings. They belong to the load-bearing walls typology, in which the resistant elements are bearing walls for the upper levels, complemented by masonry and cast iron pillars in the base levels. The characteristic number of stories of these buildings ranges from 6 to 8, and in our case all the buildings have 7 stories.

The main bearing walls correspond to the walls located in the front and back façades, the walls between buildings, and the walls that constitute the inner courtyards of the structure. For the upper levels two extra bearing walls are located between the central courtyard and each façade. These additional bearing walls are sustained by metallic pillars and girders in the base levels whose function is to allow greater clear areas for commercial activities (See Fig. 3.2).

According to their function and location in the different levels of the building, the thickness as well as the number and size of the openings present in each wall varies considerably as shown in Table 3.1.

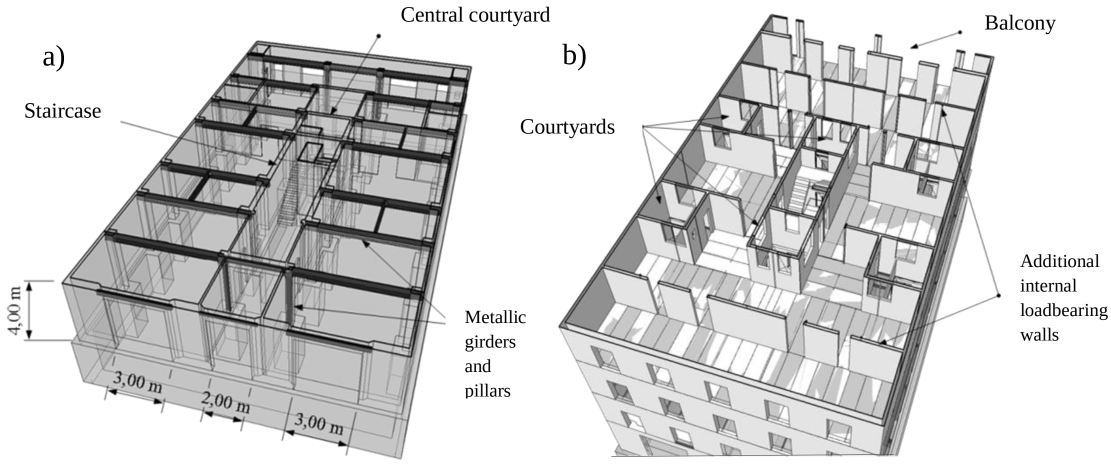


**Figure 3.2.** Isometric view of building M153. a) Base level. b) Upper levels

**Table 3.1.** Typical wall thickness of the buildings of the Eixample district

| Level | | 1 | 2, 3, … |
|---|---|---|---|
| Wall thickness [cm] | Main façade | 45-60 | 30-45 |
| | Post facade | 30-45 | 30-45 |
| | Staircases | 30 | 15 |
| | Inner bearing walls | - | 15 |
| | Intermediate bearing walls | 30 | 15 |
| | Distribution walls | - | 5 |

For the construction period of the analyzed buildings, the characteristic type of floors consisted of iron beams and brick vaults (See Fig. 3.3). Previous to this period, one way timber floors with single or overlapped wood planks and concrete topping were used. In the other hand, after this period, due to the lack of iron and steel caused by the war, reinforced concrete beams and ceramic vaults were the typical solution.

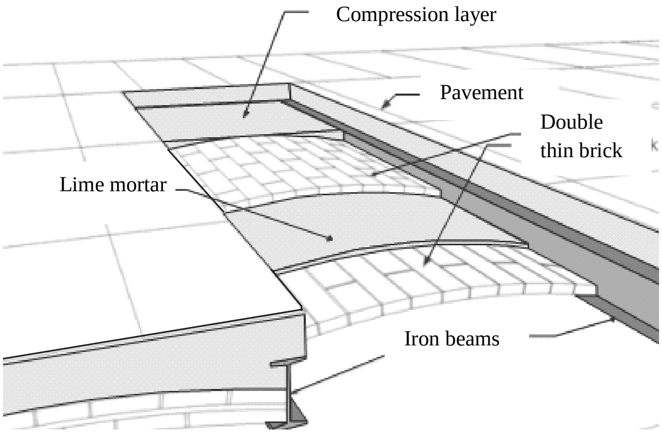


**Figure 3.3.** Floor system based on iron beams and single or double brick vaults

These buildings present big openings (doorways or windows) in their façades and inner walls, which was solved by discharging arches and lintels (See Fig. 3.2a). The materials, dimensions and number of elements used for the lintels vary according to the length of the opening and the type of wall, being wood and iron the most used. For further details of the specific architectonic features of the masonry buildings of the Eixample district, see Paricio (2008).

The modal analysis (Table 3.2) was performed for each building and the aggregate with the TREMURI software (Lagomarsino et al., 2008). For all the structures the first and second modes correspond to the translational modes, and the third mode correspond to the rotational one.

**Table 3.2.** Parameters for the deterministic and probabilistic seismic scenarios of Barcelona city

| | Mode | T[s] | mx [kg] | Mx[%] | my[kg] | My[%] | mz[kg] | Mz[%] |
|---|---|---|---|---|---|---|---|---|
| M153/ M155 | 1 | 0,54770 | 467 | 0,02 | 1872181 | 74,31 | 5 | 0,00 |
| | 2 | 0,53658 | 2197037 | 87,21 | 403 | 0,02 | 8 | 0,00 |
| | 3 | 0,46824 | 81 | 0,00 | 0 | 0,00 | 3 | 0,00 |
| A155 | 1 | 0,57124 | 17 | 0,00 | 3958285 | 75,59 | 6 | 0,00 |
| | 2 | 0,54403 | 4362142 | 83,30 | 26 | 0,00 | 2 | 0,00 |
| | 3 | 0,50208 | 165877 | 3,17 | 28 | 0,00 | 12 | 0,00 |
| M157 | 1 | 0,68759 | 1131423 | 74,28 | 0 | 0,00 | 3 | 0,00 |
| | 2 | 0,56238 | 2 | 0,00 | 1158621 | 76,07 | 11 | 0,00 |
| | 3 | 0,52485 | 242652 | 15,93 | 7 | 0,00 | 3 | 0,00 |
| M159 | 1 | 0,66808 | 1101344 | 87,26 | 4365 | 0,35 | 4 | 0,00 |
| | 2 | 0,52099 | 10408 | 0,82 | 915729 | 72,56 | 89 | 0,01 |
| | 3 | 0,49452 | 5406 | 0,43 | 77849 | 6,17 | 1 | 0,00 |

## 4. DEMAND SCENARIOS

The seismic hazard of Barcelona, which is located in a low-to-moderate seismic zone, was evaluated using deterministic and probabilistic methods. The several studies related to the definition of seismic scenarios (Ambrasseys et al., 1996; Susagna et al., 1998; Secanell et al., 2004), soil zonation (Cid, 1998), analytical formulations (Lagomarsino et al., 2002; Milutinovic et al., 2003) and their validation for Barcelona (Irizarry, 2004) have been taken into account.

The Eixample district is located in the soil zone II, one of the four different existing soil zones in the city. Each building presents two main orthogonal directions (+X and +Y). Table 4.1 shows the 5% damped elastic response spectrum parameters for both scenarios, deterministic and probabilistic, for each soil zone.

**Table 4.1.** Parameters of the 5% damped elastic response spectra for Barcelona's different soil zones

| Soil Zone | *pga* (g) | $T_B$ | $T_C$ | $B_C$ | d | $T_D$ | $B_D$ | Scenario |
|---|---|---|---|---|---|---|---|---|
| I | 0.188 | 0.10 | 0.39 | 1.91 | 1.70 | 2.30 | 0.09 | Deterministic |
| | 0.136 | 0.10 | 0.40 | 2.00 | 1.34 | 2.85 | 0.14 | Probabilistic |
| *II* | *0.194* | *0.10* | *0.22* | *2.45* | *1.43* | *2.20* | *0.09* | *Deterministic* |
| | *0.141* | *0.10* | *0.23* | *2.50* | *1.28* | *2.21* | *0.14* | *Probabilistic* |
| III | 0.169 | 0.10 | 0.22 | 2.29 | 1.40 | 2.00 | 0.10 | Deterministic |
| | 0.122 | 0.10 | 0.19 | 2.57 | 1.12 | 1.77 | 0.20 | Probabilistic |
| R | 0.100 | 0.10 | 0.23 | 2.26 | 1.12 | 1.75 | 0.23 | Deterministic |
| | 0.072 | 0.10 | 0.25 | 2.29 | 0.98 | 1.75 | 0.34 | Probabilistic |

## 5. METHODOLOGY

The analyses performed for each building in this work were developed following the guidelines of the RISK-UE Project (Milutinovic et al., 2003). The elastic demand spectrum formulations (Eqns. 5.1 to 5.4) were obtained from the adaptation and validation performed by Irizarry (2004) to the original proposal of the University of Genoa found in the WP4 of the already mentioned guidelines.

The capacity spectrum method was implemented in order to assess the capacity and fragility of the structures (ATC-40, 1996). Figure 6.1 shows the M153 capacity curves and spectra for each analysis direction, and Table 6.1 presents the corresponding results for the other analyzed structures.

$$
\frac{S_a(T)}{pga} = \begin{cases} 1 + \frac{T}{T_B}(B_C - 1) & 0 \le T \le T_B \quad (5.1) \\ B_C & T_B \le T \le T_C \quad (5.2) \\ \left[\frac{T_C}{T}\right]^d B_C & T_C \le T \le T_D \quad (5.3) \\ \left[\frac{T_D}{T}\right]^2 B_D & T \ge T_D \quad (5.4) \end{cases}
$$

The building damage states were established as proposed in the RISK-UE guidelines, identifying four different damage states: SL-*slight* ($d_{s1}$), MO-*moderate* ($d_{s2}$), SE-*severe* ($d_{s3}$) and CO-*complete* ($d_{s4}$). A non-damage state is also defined as NO-*no damage*. These damage states can be defined from the yielding ([$S_{dy}$, $S_{ay}$]) and ultimate ([$S_{du}$, $S_{au}$]) displacement parameters of the bilinear representation of the capacity spectrum as follows (Lagomarsino et al., 2002):

$$\overline{ds}_1 = 0.7S_{dy} \tag{5.5}$$
$$\overline{ds}_2 = S_{dy} \tag{5.6}$$
$$\overline{ds}_3 = S_{dy} + 0.25(S_{du} - S_{dy}) \tag{5.7}$$
$$\overline{ds}_4 = S_{du} \tag{5.8}$$

For the development of the fragility curves, the spectral displacement was used as the seismic action defining parameter. Lognormal distributions were assumed as adequate for the representation of the statistical variation (FEMA/NIBS, 1999).

$$P[ds \ge ds_i|sd] = \Phi\left[\ln\left(\frac{sd}{\overline{sd}_{ds_i}}\right)/\beta_{ds_i}\right] \tag{5.9}$$

where $\beta_{ds_i}$ is the standard deviation of the natural logarithm of the spectral displacement at which the structure reaches the damage state $d_{si}$, $\overline{sd}_{ds_i}$, is the mean value of this spectral displacement, and $\Phi$ is the normal standard cumulative function. The M153 building fragility curves for both scenarios and both analysis directions are shown in Figure 6.2. The results for all the analyzed buildings for the deterministic and probabilistic scenarios are summarized in Table 6.2 and Table 6.3, respectively.

The seismic damage of the buildings is supposed to follow a Binomial probability function, assigning for each damage state a 50% probability of reaching or exceeding that particular damage (Lantada et al., 2009).

A damage index was calculated in order to obtain an indicator of the global expected damage in the structure and its distribution. It was calculated as a normalized mean damage value defined in the next expression:

$$DI = \frac{1}{n} d_m = \frac{1}{n}\sum_{i=0}^{n} i \times P(ds_i) \tag{5.10}$$

where $n$ is the number of damage states, and $P(ds_i)$ is the probability that a damage state i occurs.

## 6. DISCUSSION OF THE RESULTS AND CONCLUSSIONS

The assessment of the seismic vulnerability and risk of the typical URM buildings of the Eixample district of Barcelona implies an evaluation via advanced methods as those proposed in the RISK-UE project.

For the purpose of this work, four isolated buildings were studied as well as one aggregate. The structures were analyzed in their two main inertia directions: +X (parallel to the street) and +Y. The buildings are aggregated in the +X direction, being this direction the shorter side for all the isolated buildings.

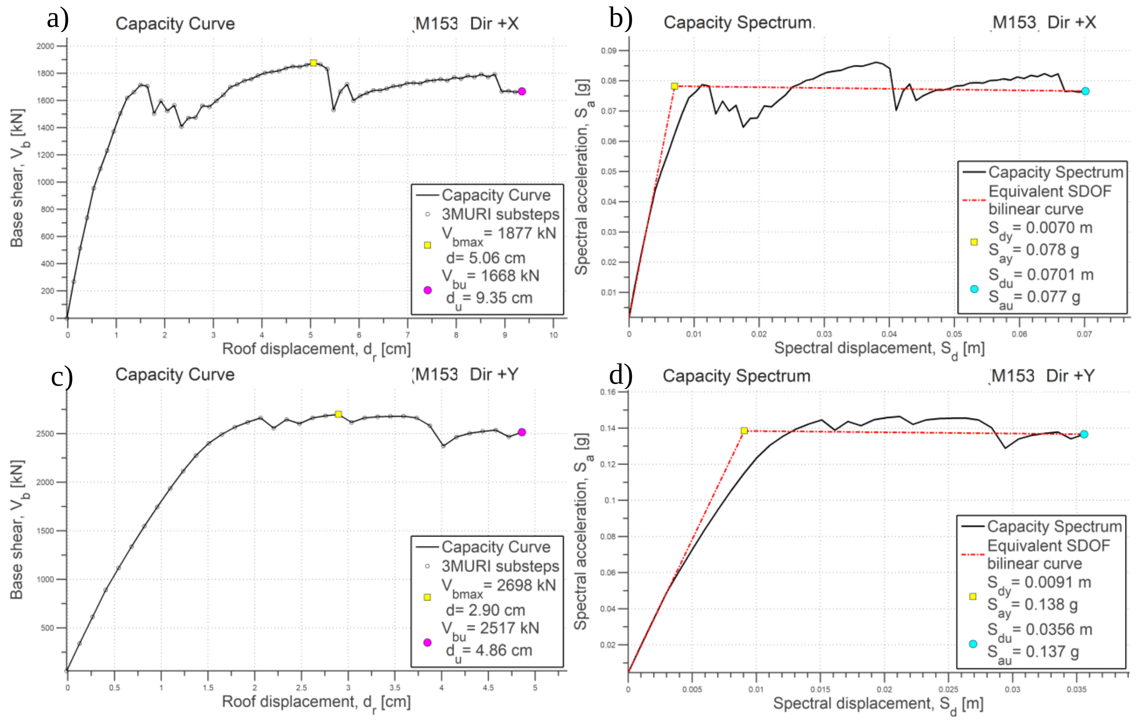


**Figure 6.1.** Capacity curves and spectra of building M153

**Table 6.1.** Capacity curves and spectra data of the analyzed buildings

| | Direction | $V_{bmax}$ [kN] | d [cm] | $V_{bu}$ [kN] | $d_u$ [cm] | $S_{dy}$ [cm] | $S_{ay}$ [g] | $S_{du}$ [cm] | $S_{au}$ [g] |
|---|---|---|---|---|---|---|---|---|---|
| M155 | +X | 1877 | 5,06 | 1668 | 9,35 | 0,70 | 0,078 | 7,01 | 0,077 |
| | +Y | 2698 | 2,90 | 2517 | 4,86 | 0,91 | 0,138 | 3,56 | 0,137 |
| A155 | +X | 3896 | 4,21 | 3213 | 6,18 | 0,70 | 0,087 | 4,72 | 0,072 |
| | +Y | 5572 | 4,69 | 5295 | 6,51 | 1,03 | 0,132 | 4,80 | 0,134 |
| M157 | +X | 883 | 8,12 | 828 | 10,51 | 0,76 | 0,058 | 7,97 | 0,062 |
| | +Y | 1757 | 2,34 | 1533 | 3,56 | 1,06 | 0,143 | 2,60 | 0,135 |
| M159 | +X | 708 | 1,67 | 670 | 2,24 | 0,68 | 0,052 | 1,72 | 0,060 |
| | +Y | 1144 | 2,40 | 1136 | 3,76 | 0,59 | 0,077 | 2,75 | 0,115 |

The accuracy in the modelling of the structures directly influences their behaviour, which is reflected on the calculations and results. In order to fulfil the lack of completeness of the floor plans of the analyzed buildings, an extensive research of the contemporary bibliography, inspection of the architectural databases and field work have been performed.

In consistency with the *pga* values (Table 4.1) of both scenarios, the deterministic scenario shows lower damage and better performance than the probabilistic scenario. Figure 6.2 shows this trend for the M153 building. The information of Table 6.2 and 6.3 is summarized in the Figure 6.3, which shows the above-mentioned tendency.

Higher damage index values are obtained for the +X direction for both scenarios, which indicates that the buildings have a better performance in the +Y direction. In the case of M159 building, this trend is less evident due to the more squared floor plant.

Except for the M159 building, the damage state probabilities for the deterministic scenario in the +X direction are located between the slight and moderate damage states, while for the +Y direction, the damage state probabilities are located between the no-damage and the slight damage states (See Fig. 6.3). These results indicate that the predominant damage for these URM buildings of Barcelona is expected to be moderate, while still having into consideration the possible values of exceedance probability related to the severe damage state.

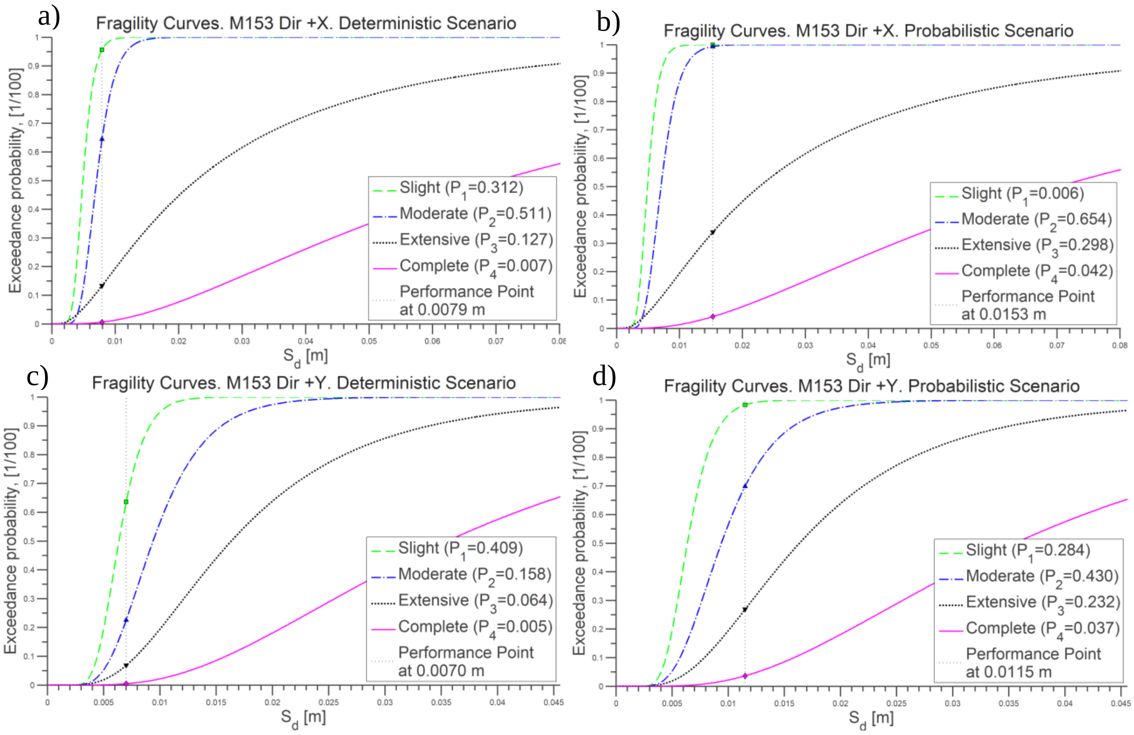


**Figure 6.2.** Fragility curves M153 building

**Table 6.2.** Deterministic Scenario. Damage states probabilities, performance point (PP) and damage index (DI). Damage states: *no damage* (NO), *slight* (SL), *moderate* (MO), *severe* (SE) and *complete* (CO)

| | | Deterministic | | | | | | |
|---|---|---|---|---|---|---|---|---|
| | Dir | NO [%] | SL [%] | MO [%] | SE [%] | CO [%] | P.P. [cm] | D. I. [%] |
| M155 | +X | 4,3 | 31,2 | 51,1 | 12,7 | 0,7 | 0,79 | 43,5 |
| | +Y | 36,4 | 40,9 | 15,8 | 6,4 | 0,5 | 0,70 | 23,4 |
| A155 | +X | 4,1 | 43,9 | 35,9 | 14,9 | 1,2 | 0,80 | 41,4 |
| | +Y | 47,7 | 34,1 | 12,9 | 5,0 | 0,3 | 0,73 | 19,1 |
| M157 | +X | 3,8 | 28,7 | 54,1 | 12,8 | 0,6 | 0,87 | 44,4 |
| | +Y | 53,3 | 37,3 | 6,8 | 2,4 | 0,2 | 0,72 | 14,7 |
| M159 | +X | 1,4 | 18,0 | 41,3 | 32,0 | 7,3 | 0,88 | 56,4 |
| | +Y | 0,6 | 24,5 | 45,7 | 25,1 | 4,1 | 0,83 | 51,9 |

**Table 6.3.** Probabilistic Scenario. Damage states probabilities, performance point (PP) and damage index (DI). Damage states: *no damage* (NO), *slight* (SL), *moderate* (MO), *severe* (SE) and *complete* (CO)

| | | Probabilistic | | | | | | |
|---|---|---|---|---|---|---|---|---|
| | Dir | NO [%] | SL [%] | MO [%] | SE [%] | CO [%] | P.P. [cm] | D. I. [%] |
| M155 | +X | 0,0 | 0,6 | 65,4 | 29,8 | 4,2 | 1,53 | 59,4 |
| | +Y | 1,7 | 28,4 | 43,0 | 23,2 | 3,7 | 1,15 | 49,7 |
| A155 | +X | 0,1 | 19,3 | 47,7 | 28,4 | 4,5 | 1,23 | 54,5 |
| | +Y | 2,7 | 36,3 | 39,7 | 18,9 | 2,4 | 1,23 | 45,5 |
| M157 | +X | 0,0 | 1,6 | 70,5 | 25,2 | 2,7 | 1,44 | 57,2 |
| | +Y | 6,0 | 33,4 | 37,2 | 20,0 | 3,4 | 1,14 | 45,4 |
| M159 | +X | 0,0 | 0,4 | 13,3 | 48,0 | 38,3 | 1,50 | 81,0 |
| | +Y | 0,0 | 2,0 | 32,9 | 45,9 | 19,2 | 1,51 | 70,6 |

With respect to the aggregate building, which is in fact the M153 building replicated, seismic performance improvements can be seen. The resulting damage indices for both scenarios and both directions are lower than those obtained for the isolated building. This differences are specially remarkable in the +Y direction. This improvement in performance for the aggregate buildings should be confirmed via stochastic studies on a higher number and larger aggregates.

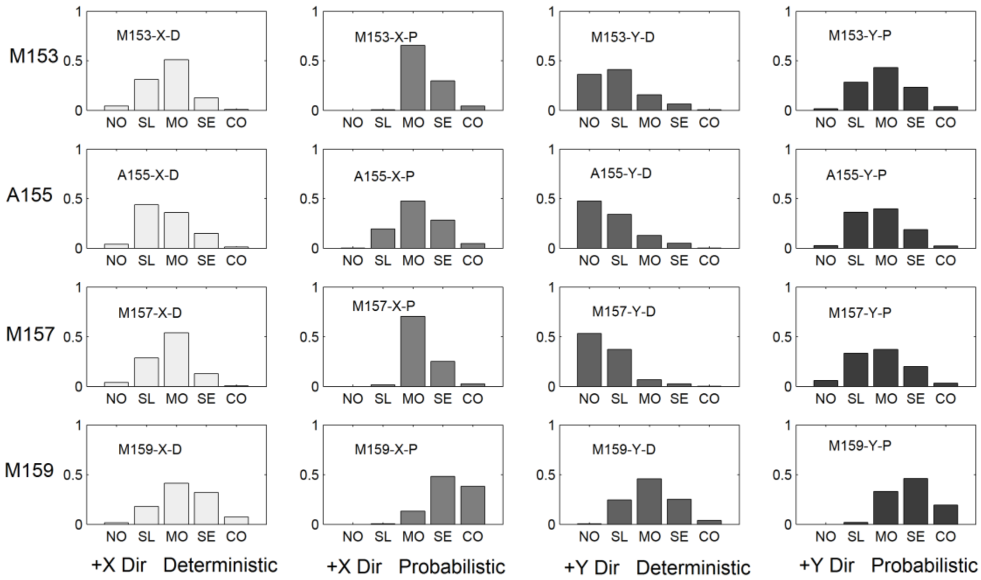


**Figure 6.3.** Damage states probabilities for each building in both directions and both scenarios

The present study, as well as previous works, shows that even though Barcelona is located in a low-to-moderate seismicity zone, it can be significantly affected due to the important vulnerability of its buildings


## AKCNOWLEDGEMENT

This work has been partially funded by the Spanish Government, by the European Commission and with FEDER funds, through the research projects: CGL2008-00869/BTE, CGL2011-23621, SEDURECCONSOLIDER-CSD2006-00060, INTERREG: POCTEFA 2007-2013/73/08, MOVE-FT7-ENV-2007-1-211590 and DESURBS-FP7-2011-261652.


## REFERENCES


Ambrasseys, N. N., Simpson, K. A., & Bommer, J. J. (1996). Prediction of horizontal response spectra in Europe. *Earthquake Engineering and Structural Dynamics*, **25**, 371-400.

ATC-40. (1996). Seismic Evaluation and Retrofit of Concrete Buildings. Applied Technology Council. Redwood City, CA: Seismic Safety Comission.

Barbat, A. H., Pujades, L. G., & Lantada, N. (2006). Performance of Buildings Under Earthquake in Barcelona, Spain. *Computer-Aided Civil and Infrastructure Engineering*, **21**, 573-593.

Barbat, A. H., Pujades, L. G., & Lantada, N. (2008). Seismic Damage Evaluation in Urban Areas Using the Capacity Spectrum Method: Application to Barcelona. *Soil Dynamics and Earthquake Engineering*, **28**, 851-865.

Carreño, M. L., Cardona, O. D., & Barbat, A. H. (2007). Urban Seismic Risk Evaluation: A Holistic Approach. *Natural Hazards*, **40**, 137-172.

Cid, J. (1998). Zonación Sísmica de la ciudad de Barcelona basada en métodos de simulación numérica de efectos locales. Barcelona, Spain: Universitat Politècnica de Catalunya.

FEMA/NIBS. (1999). HAZUZ'99 Technical Manual. Earthquake Loss Estimation Methodology. Federal-Emergency-Management-Agency and National-Institute-of-Building-Sciences, Eds.) Washington, D.C., U.S.A.

Irizarry, J. (2004). An Advanced Approach to Seismic Risk Assessment. Application to the Cultural Heritage

and the Urban System Barcelona. Dpto. Ingeniería del Terreno, Cartográfica y Geofísica. Barcelona, Spain: Universidad Politécnica de Cataluña.
Jiménez, M. J., Giardini, D., Grünthal, G. A., & SESAME-WorkingGroup. (2001). Unified Seismic Hazard Modelling throughout the Mediterranean Region. *Bolletino di Geofisica Teorica ed Applicata*, **42:1-2**, 3-18.
Lagomarsino, S., Galasco, A., & Penna, A. (2002). Pushover and dynamic analysis of URM buildings by means of a non-linear macro-element model. In R.-U. project (Ed.), *International Conference on Earthquake Loss Estimation and Risk Reduction. Bucharest*.
Lagomarsino, S., Galasco, A., Penna, A., & Cattari, S. (2008). TREMURI: Seismic Analysis Program for 3D Masonry Buildings (User Guide). Technnical Report. (U. o. Genoa, Ed.) Genoa, Italy.
Lantada, N. (2007). Evaluación del Riesgo Sísmico Mediante Métodos Avanzados y Técnicas GIS. Aplicación a Barcelona. Barcelona, Spain: Universidad Politécnica de Cataluña.
Lantada, N., Pujades, L., Barbat, A. (2009). Vulnerabitliy index and capacity spectrum based methods for urban seismic risk evaluation. A comparison. *Natural Hazards*, **51**, 501-524.
Milutinovic, Z. V., & Trendafiloski, G. S. (2003). WP4: Vulnerability of Current Buildings. In R.-U. Project, An advanced approach to earthquake risk scenarios with applications to different European towns.
Paricio Casademunt, A. (2008). Secrets d'un sistema constructiu L'Eixample. Barcelona, Spain: Edicions UPC.
Pujades, L. G., Barbat, A. H., González-Drigo, J. R., Ávila, J., & Lagomarsino, S. (2012). Seismic performance of a block of buildings representative of the typical construction in the Eixample district in Barcelona (Spain). *Bulletin of Earthquake Engineering*, **10:1**, 331-349.
Secanell, R., Goula, X., Susagna, T., Fleta, J., & Roca, A. (2004). Seismic hazard zonation of Catalonia, Spain, integrating uncertainties. *Journal of Seismology*, **8**, 24-40.
Susagna, T., & Goula, X. (1998). Atlas Sísmic de Catalunya. In I. C. Catalunya.